ACS Catalysis
LETTER
pubs.acs.org/acscatalysis

Synthesis and Hydrodeoxygenation Properties of Ruthenium Phosphide Catalysts

Richard H. Bowker,[†] Mica C. Smith,[†] Melissa L. Pease,[†] Karla M. Slenkamp,[†] Libor Kovarik,[‡] and Mark E. Bussell*[,†]

[†]Department of Chemistry and Advanced Materials Science and Engineering Center, Western Washington University, 516 High Street, MS-9150, Bellingham, Washington 98225, United States

[‡]Environmental Molecular Sciences Laboratory, Pacific Northwest National Laboratory, P.O. Box 999, K8-93, Richland, Washington 99352, United States

S *Supporting Information*

ABSTRACT: Ru_2P/SiO_2 and RuP/SiO_2 catalysts were prepared by the temperature-programmed reduction (TPR) of uncalcined precursors containing hypophosphite ion ($H_2PO_2^-$) as the phosphorus source. The Ru_2P/SiO_2 and RuP/SiO_2 catalysts had small average particle sizes (~4 nm) and high CO chemisorption capacities (90−110 μmol/g). The Ru phosphide catalysts exhibited similar or higher furan (C_4H_4O) hydrodeoxygenation (HDO) activities than did a Ru/SiO_2 catalyst, and the phosphide catalysts favored C_4 hydrocarbon products while the Ru metal catalyst produced primarily C_3 hydrocarbons.

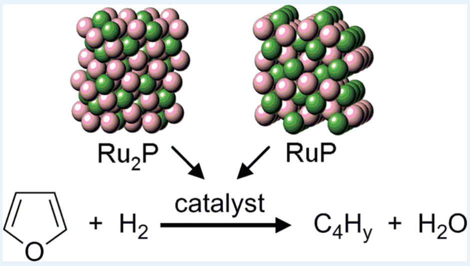

KEYWORDS: hydrodeoxygenation, HDO, furan, ruthenium, ruthenium phosphide

With a goal of decreasing our dependence on fossil fuels, increasing attention is being focused on the conversion of cellulosic biomass to liquid transportation fuels. One technology for accomplishing this conversion is a two-step process involving fast pyrolysis of the biomass feedstock followed by catalytic upgrading of the resulting bio-oil fraction to biofuel.[1−3] Bio-oils are complex chemical mixtures that contain significant amounts of oxygen (35−40 wt %); the high oxygen content results in deleterious fuel properties including low energy density, high viscosity, and high acidity that make bio-oils unsuitable as fuels unless they are upgraded.[2]

Hydrodeoxygenation (HDO) is a catalytic process whereby the oxygen content can be lowered in order to improve the properties of fuels derived from bio-oils. Many HDO studies of model compound or bio-oil feeds have utilized commercial $Co-Mo/Al_2O_3$ and $Ni-Mo/Al_2O_3$ catalysts developed for the hydrotreatment of crude oil feeds.[2−9] Sulfide phase decomposition and carbon deposition have been identified as mechanisms for catalyst deactivation for $Co-Mo/Al_2O_3$ and $Ni-Mo/Al_2O_3$ catalysts during HDO processing.[9,10] Because of the problems encountered in using sulfide catalysts for HDO of bio-oils, there has been an upsurge in research focused on the development of other classes of HDO catalysts, including noble metals,[10−15] Ni and Ni alloys,[16−18] metal carbides,[19,20] metal nitrides,[19,21] amorphous metal−boron alloys,[22−24] and metal phosphides.[25,26] In the cases in which these nonsulfide catalysts were compared to commercial $Co-Mo/Al_2O_3$ and $Ni-Mo/Al_2O_3$ catalysts (or other sulfide catalysts), some had HDO activities similar to or higher than those of the sulfide catalysts.[10,12,25,26]

Two recent studies have shown molybdenum phosphide (MoP) and nickel phosphide (Ni_2P) catalysts to be more active than metal sulfide catalysts for HDO of model compounds.[25,26] Also of importance to the current report, the synthesis of silica-supported noble metal phosphides (e.g., Rh_2P, Ru_2P) has recently been described, and these materials have been observed to be more active than the corresponding noble metals for the hydrodesulfurization (HDS) of dibenzothiophene.[27,28] The current study describes the synthesis and HDO properties of silica-supported ruthenium phosphide (Ru_2P, RuP) catalysts, which were observed to have similar or higher furan HDO activities than Ru metal and to be substantially more active than a commercial $Co-Mo/Al_2O_3$ catalyst. Further, the incorporation of P into Ru dramatically shifted the HDO selectivity from C_3 hydrocarbons for Ru metal to C_4 hydrocarbons for Ru_2P and RuP.

Ru_2P/SiO_2 and RuP/SiO_2 catalysts were prepared by the temperature-programmed reduction (TPR) of uncalcined precursors having P/Ru molar ratios of 0.86 and 1.1, respectively. The uncalcined precursors were prepared by the sequential impregnation of silica with ruthenium chloride ($RuCl_3$) and ammonium hypophosphite ($NH_4H_2PO_2$). The synthesis procedure, which is described in detail in the Experimental Methods, was adapted from syntheses of unsupported and supported metal phosphides (e.g., Ni_2P) reported by others that utilized the

Received: May 9, 2011
Revised: June 24, 2011
Published: July 06, 2011

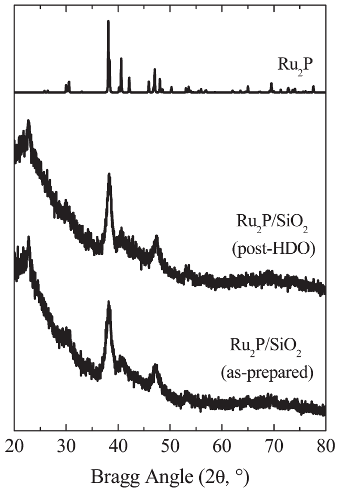

Figure 1. XRD patterns for as-prepared and HDO-tested Ru_2P/SiO_2 catalysts.

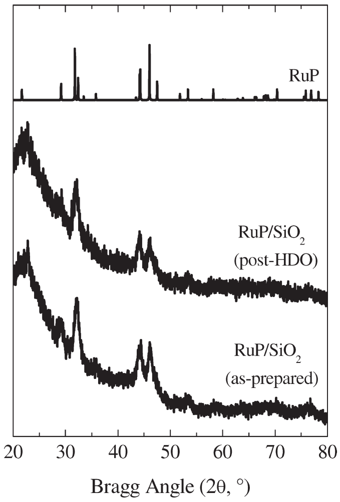

Figure 2. XRD patterns for as-prepared and HDO-tested RuP/SiO_2 catalysts.

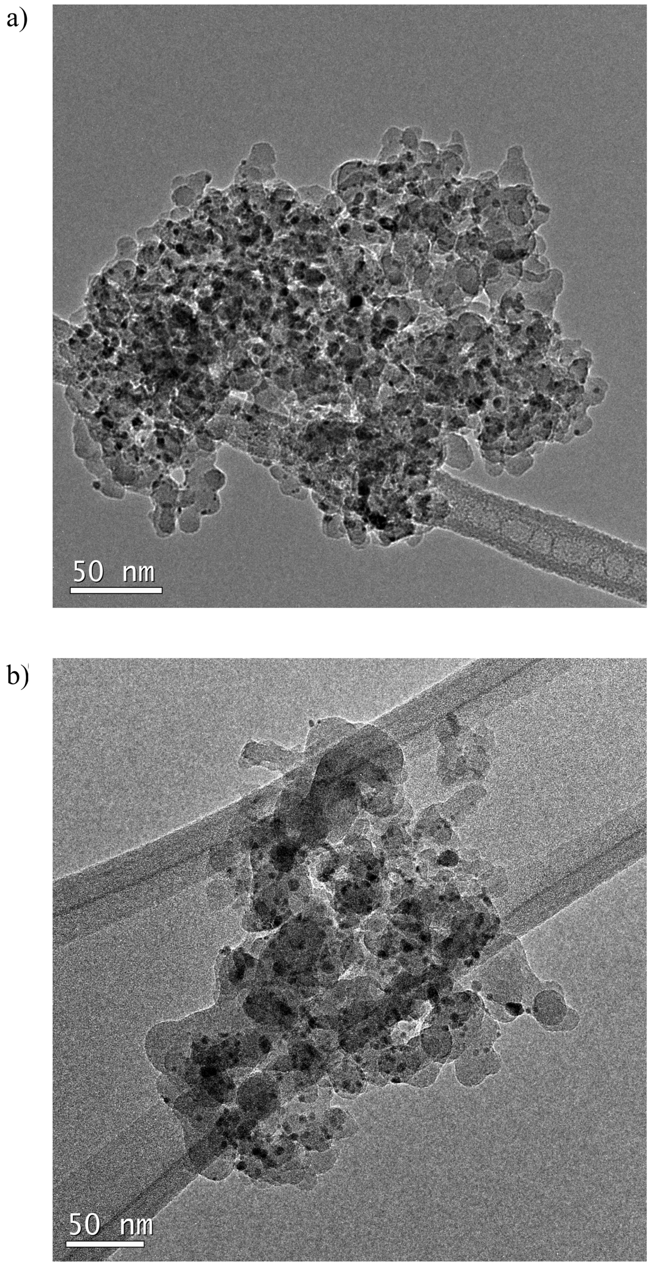

Figure 3. TEM images of the (a) Ru_2P/SiO_2 and (b) RuP/SiO_2 catalysts.

hypophosphite ion ($H_2PO_2^-$) as the P source.[29−31] While in these studies the metal phosphide phase was prepared by decomposition of the hypophosphite precursor in an inert gas, the Ru_2P/SiO_2 (11.5 wt % Ru) and RuP/SiO_2 (11.4 wt % Ru) catalysts prepared in the current study were synthesized by reducing the uncalcined precursors in flowing hydrogen at 773 K. X-ray diffraction (XRD) patterns for the as-prepared Ru_2P/SiO_2 and RuP/SiO_2 catalysts are shown in Figures 1 and 2, respectively. The XRD pattern for the silica-supported Ru_2P compares well with that of a Ru_2P reference pattern (card no. 89−3031).[32] Using the Scherrer equation and the {112} reflection at 38.2°, an average Ru_2P crystallite size of 8 nm was calculated for the Ru_2P/SiO_2 catalyst. A transmission electron microscopy (TEM) image of the catalyst shown in Figure 3 reveals well dispersed Ru_2P particles on the silica support having an average particle size of 4.1 ± 1.9 nm (see Supporting Information). The substantially smaller Ru_2P particle size determined by TEM relative to that from XRD is likely due to the fact that the smallest Ru_2P particles are below the detection limit for XRD but contribute to the average TEM particle size. Energy dispersive X-ray (EDX) analysis of the Ru_2P/SiO_2 catalyst yielded a composition of $Ru_{2.5}P_{1.0}$, which is Ru-rich relative to the expected bulk stoichiometry. The TPR synthesis of a 5 wt % Ru_2P/SiO_2 catalyst from a ruthenium phosphate precursor (P/Ru = 0.98) was recently reported by Kanda et al.[28] Despite the lower loading of this catalyst (5 wt %) compared to the Ru_2P/SiO_2 catalyst prepared in the current study, a larger average Ru_2P crystallite size of 22 nm was reported, which is likely due to the precursor being calcined and the higher TPR synthesis temperature used (923 K).

The XRD pattern for the RuP/SiO_2 catalyst is in good agreement with the XRD pattern for unsupported RuP shown in Figure 2. An average RuP crystallite size of 10 nm was calculated

Table 1. Properties of Ru Phosphide and Comparison Catalysts

catalyst	BET surface area (m^2/g)	chemisorption capacity (μmol CO/g)	furan HDO activity[a] (nmol furan/g·s)	turnover frequency (s^{-1})
Ru_2P/SiO_2	150	110	12390	0.11
RuP/SiO_2 (hypo.)	142	92	3860	0.042
RuP/SiO_2 (phos.)	137	90	5720	0.064
Ru/SiO_2	160	72	4470	0.064
25 wt % Ni_2P/SiO_2	118	64	1610	0.025
Co−Mo/Al_2O_3	230	66[b]	270	0.0041

[a] HDO activity after 48 h on-stream at 673 K. [b] Oxygen chemisorption (μmol O_2/g) at 196 K.

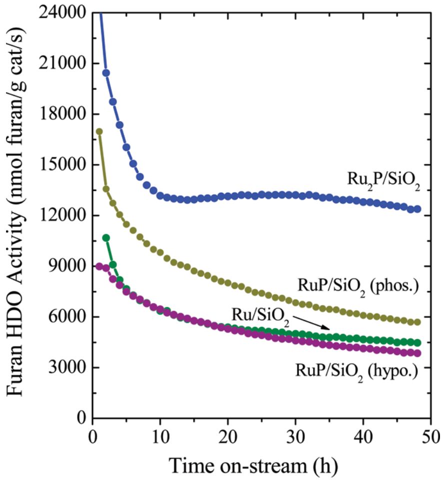

Figure 4. Furan HDO activity vs time for the Ru_2P/SiO_2, RuP/SiO_2, and Ru/SiO_2 catalysts.

using the Scherrer equation and the {011} reflection at 31.8°. A TEM image of the catalyst shown in Figure 3 reveals well dispersed RuP particles on the silica support having an average particle size of 4.1 ± 1.8 nm (see Supporting Information). The discrepancy between the average RuP particle size from TEM and the average crystallite size from XRD is rationalized as explained above for the Ru_2P/SiO_2 catalyst. EDX analysis of the RuP/SiO_2 catalyst yielded a composition of $Ru_{1.3}P_{1.0}$, which is Ru-rich relative to the expected bulk stoichiometry. For comparison purposes, a second RuP/SiO_2 catalyst was prepared by TPR of a silica-supported ruthenium phosphate precursor (P/Ru = 1.0) at 973 K. The XRD pattern for this RuP/SiO_2 catalyst is shown in Figure S1 of the Supporting Information. A small peak in the XRD pattern at 38.4° suggests a minor Ru_2P impurity was present in the catalyst. Using the Scherrer equation, an average RuP crystallite size of 29 nm was calculated for the RuP/SiO_2 catalyst prepared from the Ru phosphate precursor. The larger average RuP crystallite size for this catalyst relative to the RuP/SiO_2 catalyst prepared from the hypophosphite precursor is not surprising given the higher TPR temperature needed to reduce the phosphate precursor (973 K). The synthesis of unsupported RuP by hydrogen reduction of $RuP_2O_7 \cdot 2H_2O$ at 873 K was reported previously,[33] as had the preparation of RuP in a silica xerogel by hydrogen reduction of a single source precursor at 973 K.[34] The RuP−silica xerogel (15 wt % RuP) had an average RuP crystallite size of 5 nm, but its catalytic properties were not reported.[34] The BET surface areas and CO chemisorption capacities for the Ru_2P/SiO_2 and RuP/SiO_2 catalysts prepared in the current study, along with values for three comparison catalysts, are listed in Table 1.

To make an initial assessment of the properties of Ru_2P and RuP catalysts for upgrading bio-oils via HDO processing, furan HDO activity measurements were carried out for the Ru_2P/SiO_2 and RuP/SiO_2 catalysts as well as for a number of comparison catalysts, including a commercial Co−Mo/Al_2O_3 catalyst. The furan HDO activity at 673 K is plotted versus time in Figure 4 for the Ru_2P/SiO_2 and RuP/SiO_2 catalysts, as well as for a Ru/SiO_2 catalyst having a similar Ru loading as the phosphide catalysts. The Ru_2P/SiO_2, RuP/SiO_2, and Ru/SiO_2 catalysts exhibited a trend of decreasing HDO activity vs time during the 48 h test period on-stream. However, the activity of the Ru_2P/SiO_2 catalyst showed a slower decline than the other catalysts after 10 h on-stream, with its HDO activity decreasing just 6% between 10 and 48 h on-stream. The RuP/SiO_2 catalysts prepared from the hypophosphite (RuP/SiO_2 (hypo.)) and phosphate (RuP/SiO_2 (phos.)) precursors displayed similar activity trends with time, but the RuP/SiO_2 (phos.) catalyst was ∼1.5 times more active. The Ni_2P/SiO_2 and Co−Mo/Al_2O_3 catalysts also exhibited decreasing HDO activities vs time on-stream. The HDO activities and turnover frequencies (TOFs) of the Ru_2P/SiO_2, RuP/SiO_2 and Ru/SiO_2 catalysts after 48 h on-stream are compared to those of a 25 wt % Ni_2P/SiO_2 catalyst and a commercial Co−Mo/Al_2O_3 catalyst in Table 1. The HDO activities decreased in the order: Ru_2P/SiO_2 > RuP/SiO_2 (phos.) > Ru/SiO_2 > RuP/SiO_2 (hypo.) > Ni_2P/SiO_2 > Co−Mo/Al_2O_3. The Ru_2P/SiO_2 catalyst is significantly more active than the other catalysts investigated; it is nearly three times more active than the Ru/SiO_2 catalyst and two and three times more active than the RuP/SiO_2 catalysts prepared from the phosphate and hypophosphite precursors, respectively. On a TOF basis, the Ru_2P/SiO_2 catalyst is nearly twice as active as the RuP/SiO_2 (phos.) and Ru/SiO_2 catalysts and nearly three times as active as the RuP/SiO_2 (hypo.) catalyst. The range of HDO activities observed for the Ru, Ru_2P, and RuP catalysts, as well as for additional catalysts prepared from P/Ru ratios that yielded mixed phases, indicates a strong dependence of catalyst activity on composition. This may explain the higher activity for the RuP/SiO_2 (phos.) catalyst, which was prepared from a precursor having P/Ru =1 and contained a small Ru_2P impurity, than for the RuP/SiO_2 (hypo.) catalyst that was prepared from a precursor having P/Ru = 1.1 and was phase pure RuP. Additional studies will be needed to probe the strong dependence of HDO activity on Ru phosphide composition.

The Ru_2P/SiO_2, RuP/SiO_2, and Ru/SiO_2 catalysts were over 1 order of magnitude more active than the commercial Co−Mo/Al_2O_3 catalyst for furan HDO on mass and TOF bases. The higher activity of the Ru/SiO_2 catalyst compared to the Co−Mo/Al_2O_3 catalyst is consistent with the findings of Wildschut et al.,[12] who reported Ru/C and Ru/TiO_2 catalysts to be more active than Co−Mo/Al_2O_3 and Ni−Mo/Al_2O_3 catalysts for HDO of a fast pyrolysis bio-oil. The Ru_2P/SiO_2 and RuP/SiO_2 catalysts also compared favorably with a 25 wt % Ni_2P/SiO_2 catalyst for the HDO of furan. The Ru_2P/SiO_2 and RuP/SiO_2 (phos.) catalysts were 7.7 and 3.5 times more active than the Ni_2P/SiO_2 catalyst on a mass basis, respectively, and 4.4 and 2.6

Table 2. HDO Product Selectivities of Ru Phosphide and Comparison Catalysts

catalyst	Ru_2P/ SiO_2	RuP/ SiO_2 (hypo.)	RuP/ SiO_2 (phos.)	Ru/ SiO_2	Ni_2P/ SiO_2	Co−Mo/ Al_2O_3
C_3H_y	17	11	11	89	37	7
1-butene	6	8	4	0	5	21
cis-2-butene	8	11	5	0	6	16
trans-2-butene	11	13	6	0	5	13
butane	58	57	74	11	47	43

Scheme 1. Reaction Pathways for Furan HDO

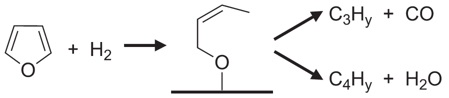

times more active on a TOF basis. Oyama and co-workers[26] recently reported catalyst activities for HDO of 2-methoxyphenol (also called guaiacol) for a number of silica-supported metal phosphides and determined the following order of activity: $Ni_2P/SiO_2 > Co_2P/SiO_2 > Fe_2P/SiO_2 > WP/SiO_2 > MoP/SiO_2$. The metal phosphide catalysts were more active than a commercial Co−Mo/Al_2O_3 catalyst. In the current study, the 25 wt % Ni_2P/SiO_2 catalyst was observed to be dramatically more active than a commercial Co−Mo/Al_2O_3 catalyst, but it was also significantly less active than Ru metal and Ru phosphide catalysts.

The furan HDO product selectivities after 24 h on-stream for the Ru_2P/SiO_2, RuP/SiO_2, and Ru/SiO_2 catalysts are listed in Table 2. The product selectivities differ significantly for the Ru phosphide and Ru metal catalysts, with the Ru_2P/SiO_2 and RuP/SiO_2 catalysts strongly favoring C_4 hydrocarbon products and the Ru/SiO_2 catalyst strongly favoring C_3 hydrocarbon products. C_4 hydrocarbons were also the major products for furan HDO over the Ni_2P/SiO_2 and commercial Co−Mo/Al_2O_3 catalysts, but the Ni_2P/SiO_2 catalyst produced significantly more C_3 hydrocarbons than did the Ru_2P/SiO_2 and RuP/SiO_2 catalysts. No tetrahydrofuran (C_4H_8O) or butadiene (C_4H_6) were detected in the reactor effluent for any of the catalysts tested. On the basis of a study of furan HDO over a commercial Co−Mo/Al_2O_3 catalyst, Furimsky[4] proposed two pathways for oxygen removal from a ring-opened intermediate as shown in Scheme 1. C_4 hydrocarbons are produced by hydrogenolysis of the remaining C−O bond in the ring opened intermediate, while the C_3 hydrocarbons are produced by a decarbonylation pathway in which the C−C bond adjacent to the O atom is cleaved to give a C_3 hydrocarbon and carbon monoxide. Schulz and Rahman[35] observed a strong dependence of the product selectivity (C_3 vs C_4 hydrocarbons) on the hydrogen pressure for furan HDO over a Co−Mo/Al_2O_3 catalyst. The proportion of C_3 hydrocarbons in the products decreased significantly with increasing hydrogen pressure, which the authors attributed to the availability of hydrogen on the catalyst surface. The decarbonylation pathway requires less hydrogen than does the hydrogenolysis pathway, which is consistent with the dependence of the C_3/C_4 selectivity on hydrogen pressure observed by these authors.[35] The large differences in C_3 vs C_4 selectivity observed for the Ru phosphide and Ru metal catalysts in the current study could, therefore, be due to increased hydrogen availability on the Ru phosphide catalysts relative to Ru metal. Whiffen and Smith[25] compared unsupported MoP, MoS_2, and MoO_x ($x = 2, 3$) for the HDO of 4-methylphenol and observed the MoP to have the highest selectivity toward hydrogenated products of the different catalysts. Alternatively, the different furan HDO product selectivities observed for the Ru phosphide and Ru metal catalysts could be due to differences in the adsorption geometries of a key reaction intermediate such as the ring-opened species shown in Scheme 1. Resasco and co-workers[36] recently observed that the selectivity toward the decarbonylation pathway for the conversion of aldehydes on Pd/SiO_2 catalysts could be greatly reduced by incorporating Cu to form Cu−Pd/SiO_2 catalysts. The authors proposed that the incorporation of Cu resulted in destabilization of an adsorbed intermediate that reacted by the decarbonylation pathway. It is possible that the incorporation of P into Ru to form Ru_2P and RuP had a similar effect on the reactivity of an adsorbed intermediate in the furan HDO reaction pathway, decreasing the selectivity toward decarbonylation products. Vibrational spectroscopy of adsorbed acetone on the Ru(111) surface revealed that acetone adsorbed in a η^2(C, O)-geometry predominated on the clean surface, while an η^1(O)-species predominated on a partially oxygen covered surface ($\theta_O = 0.25$).[37,38] Upon heating in vacuum, the η^1(O)-species desorbed from the surface while the η^2(C, O)-species underwent decarbonylation to give CO, CH_x fragments, and hydrogen. The authors attributed the increased stabilization of the η^1(O)-species on the partially oxygen covered Ru(001) surface to increased Lewis acidity at the surface. Phosphorus in Ru_2P and RuP may play a similar role, increasing the Lewis acidity at the surface, resulting in stabilization of a ring-opened species having a η^1(O)-geometry (see Scheme 1) on these catalysts, while an η^2(C,O)-species dominates on the Ru/SiO_2 catalyst. The η^1(O)-intermediate would be expected to lead to C−O bond cleavage and C_4 products, as observed for the Ru_2P/SiO_2 and RuP/SiO_2 catalysts, while the η^2(C, O)-intermediate would be expected to favor the decarbonylation pathway to yield C_3 products as observed for the Ru/SiO_2 catalyst.

XRD patterns for the HDO-tested Ru_2P/SiO_2 and RuP/SiO_2 catalysts prepared from the hypophosphite precursors are shown in Figures 1 and 2, respectively, and in Supporting Information Figure S1 for the RuP/SiO_2 catalyst prepared from the phosphate precursor. The XRD pattern for the HDO-tested catalysts prepared from the hypophosphite precursors showed no evidence for change in the phase purity or average crystallite size compared to the as-prepared catalysts. The XRD pattern for the HDO-tested RuP/SiO_2 catalyst prepared from the phosphate precursor exhibited narrower peaks relative to the as-prepared catalyst, which is indicative of an increased average RuP crystallite size (35 nm), and an increased peak intensity at 38.3°, suggesting a slightly increased Ru_2P impurity. Carbon and sulfur analysis results for the commercial Co−Mo/Al_2O_3 catalyst showed a substantial loss of sulfur occurred during HDO testing (as-prepared, 7.23 wt % S; HDO-tested, 3.20 wt % S), as well as significant deposition of carbon onto the catalyst (as-prepared, 0.10 wt % C; HDO-tested, 8.30 wt % C). The carbon content for the HDO-tested Co−Mo/Al_2O_3 catalyst is similar to the values of 6.1−7.5 wt % C reported by others following HDO testing.[10,39] The decomposition of the sulfide phase and the accumulation of carbon on the Co−Mo/Al_2O_3 catalyst were likely responsible for the rapid catalyst deactivation observed during HDO testing. Carbon analyses of the HDO-tested Ru_2P/SiO_2,

RuP/SiO_2, Ni_2P/SiO_2, and Ru/SiO_2 catalysts showed relatively low C contents for these catalysts (0.5−1.0 wt % C). At this time, it is unclear what role, if any, carbon deposition may play in the deactivation of the metal phosphide and Ru metal catalysts during the furan HDO measurements.

EXPERIMENTAL METHODS

The Ru_2P/SiO_2 and RuP/SiO_2 catalysts were prepared by TPR of uncalcined precursors having P/Ru molar ratios of 0.86 and 1.1, respectively. The nominal Ru loadings of the Ru_2P/SiO_2 and RuP/SiO_2 catalysts based on the P/Ru molar ratios of the precursors are 11.5 and 11.4 wt % Ru, respectively. On the basis of the stoichiometry of the Ru phosphides, these Ru loadings correspond to Ru_2P and RuP loadings of 14 and 15 wt %, respectively, on the silica support. A solution of 0.699 g $RuCl_3 \cdot 3H_2O$ (Pressure Chemical) was impregnated onto 2.00 g of SiO_2 (Cab-O-Sil, M-7D grade, 200 m^2/g), followed by drying of the impregnated support at 383 K. Solutions containing 0.0372 and 0.0483 g $NH_4H_2PO_2$ (Fluka Analytical, >97%) were impregnated onto 0.500 g samples of the dried $RuCl_3/SiO_2$, followed by drying at 340 K, to give precursors having P/Ru molar ratios of 0.86 and 1.1, respectively. Samples of the two precursors were then reduced in a 100 mL/min H_2 (Airgas, 99.999%) flow with heating from room temperature to 773 K at a rate of 5 K/min followed by holding at 773 K for 1 h. Following cooling to room temperature in continued H_2 flow, the Ru_2P/SiO_2 and RuP/SiO_2 catalysts were passivated in a 1.0 mol % O_2/He (Airgas) mixture at 60 mL/min for 2 h. A sample of the uncalcined $RuCl_3/SiO_2$ precursor was used to prepare the reduced Ru/SiO_2 catalyst (13.5 wt % Ru) as described below. The synthesis of the RuP/SiO_2 (phos.) catalyst is described in the Supporting Information.

The catalysts prepared in this study were characterized by XRD, TEM, BET surface area, and CO (or O_2) chemisorption measurements as well as C and S analyses as described elsewhere.[27] Furan HDO activity measurements were carried out at a reaction temperature of 673 K using a reactor feed consisting of a 8.2 mol % furan/H_2 mixture, prepared by passing a 50 mL/min flow of H_2 through two glass bubblers containing furan at 250 K. The metal phosphide and Ru metal catalysts were pretreated by degassing in He (50 mL/min) at room temperature for 30 min and then heating from room temperature to 650 K in 1 h in a 50 mL/min flow of H_2 and holding at 650 K for 2 h. The Co−Mo/Al_2O_3 catalyst was subjected to a sulfidation pretreatment in which it was heated from room temperature to 650 K in 1 h in a 50 mL/min flow of a 3.0 mol % H_2S/H_2 mixture and then held at this temperature for 2 h. Following pretreatment, the catalyst samples were heated to the reaction temperature of 673 K and the flow was switched to the furan/H_2 reactor feed (50 mL/min). The gas effluent was sampled at 1 h intervals and analyzed by gas chromatography (GC) using a flame ionization detector. The furan conversions were used to calculate the HDO activities (nmol furan/g cat s) for the different catalysts.

ASSOCIATED CONTENT

Ⓢ **Supporting Information.** The synthesis procedure for the RuP/SiO_2 (phos.) catalyst and XRD patterns of as-prepared and HDO-tested RuP/SiO_2 (phos.) catalysts, and high-angle annular dark-field (HAADF) STEM images of the Ru_2P/SiO_2 and RuP/SiO_2 catalysts used to calculate average particle sizes. This material is available free of charge via the Internet at http://pubs.acs.org.

AUTHOR INFORMATION

Corresponding Author

*Phone: 360-650-3145. Fax: 360-650-2826. E-mail: Mark.Bussell@wwu.edu.

Funding Sources

This research was supported by the National Science Foundation under grant number CHE-0809433.

ACKNOWLEDGMENT

The TEM imaging was performed at the William R. Wiley Environmental Molecular Sciences Laboratory (EMSL), a DOE User Facility operated by Battelle for the DOE Office of Biological and Environmental Research. Pacific Northwest National Laboratory is operated for the DOE under contract DE-AC06-76RLO 1830. We acknowledge ConocoPhillips (Ferndale Refinery) for providing access to the LECO SC-144DR sulfur and carbon analyzer.

REFERENCES

(1) Mohan, D.; Pittman, C. U., Jr.; Steele, P. H. *Energy Fuels* **2006**, *20*, 848.

(2) Huber, G. W.; Iborra, S.; Corma, A. *Chem. Rev.* **2006**, *106*, 4098.

(3) Elliott, D. C. *Energy Fuels* **2007**, *21*, 1792.

(4) Furimsky, E. *Appl. Catal.* **1983**, *6*, 159.

(5) Gevert, B. S.; Otterstedt, J.-E.; Massoth, F. E. *Appl. Catal.* **1987**, *31*, 119.

(6) Furimsky, E. *Appl. Catal., A* **2000**, *199*, 147.

(7) Bunch, A. Y.; Ozkan, U. S. *J. Catal.* **2002**, *206*, 177.

(8) Senol, O. I.; Ryymin, E.-M.; Viljava, T.-R.; Krause, A. O. I. *J. Mol. Catal. A: Chem.* **2007**, *277*, 107.

(9) Gandarias, I.; Barrio, V. L.; Requies, J.; Araia, P. L.; Cambra, J. F.; Guemez, M. B. *Int. J. Hydrogen Energy* **2008**, *33*, 3485.

(10) Gutierrez, A.; Kaila, R. K.; Honkela, M. L.; Slioor, R.; Krause, A. O. I. *Catal. Today* **2009**, *147*, 239.

(11) Bejblova, M.; Zamostny, P.; Cerveny, L.; Cejka, J. *Appl. Catal., A* **2005**, *296*, 169.

(12) Wildschut, J.; Mahfud, F. H.; Venderbosch, R. H.; Heeres, H. J. *Ind. Eng. Chem.* **2009**, *48*, 10324.

(13) Yakovlev, V. A.; Khromova, S. A.; Sherstyuk, O. V.; Dundich, V. O.; Ermakov, D. Y.; Novopashina, V. M.; Lebedev, M. Y.; Bulavchenko, O.; Parmon, V. N. *Catal. Today* **2009**, *144*, 362.

(14) Li, N.; Huber, G. W. *J. Catal.* **2010**, *270*, 48.

(15) Hong, D.-Y.; MIller, S. J.; Agrawal, P. K.; Jones, C. W. *Chem. Commun.* **2010**, *46*, 1038.

(16) Zhao, C.; Kou, Y.; Lemonidou, A. A.; Li, X.; Lercher, J. A. *Chem. Commun.* **2010**, *46*, 412414.

(17) Xu, Y.; Wang, T.; L., M.; Zhang, Q.; Liang, W. *Appl. Energy* **2010**, *87*, 2886.

(18) Dundich, V. O.; Khromova, S. A.; Ermakov, D. Y.; Lebedev, M. Y.; Novopashina, V. M.; Sister, V. G.; Yakimchuk, A. I.; Yakovlev, V. A. *Kinet. Catal.* **2010**, *51*, 704.

(19) Ramanathan, S.; Oyama, S. T. *J. Phys. Chem.* **1995**, *99*, 16365.

(20) Zhang, W.; Zhang, Y.; Zhao, L.; Wei, W. *Energy Fuels* **2010**, *24*, 2052.

(21) Monnier, J.; Sulimma, H.; Dalai, A.; Caravaggio, G. *Appl. Catal., A* **2010**, *382*, 176.

(22) Wang, W.; Yang, Y.; Luo, H.; Liu, W. *Catal. Commun.* **2009**, *11*, 100.

(23) Wang, W.; Yang, Y.; Luo, H.; Liu, W. *React. Kinet. Catal. Lett.* **2010**, *101*, 105.

(24) Wang, W.; Yang, Y.; Luo, H.; Liu, W. *Catal. Commun.* **2010**, *11*, 803.

(25) Whiffen, V. M.; Smith, K. J. *Energy Fuels* **2010**, *24*, 4728.

(26) Zhao, H. Y.; Li, D.; Bui, P.; Oyama, S. T. *Appl. Catal., A* **2011**, *391*, 305.

(27) Hayes, J. R.; Bowker, R. H.; Gaudette, A. F.; Smith, M. C.; Moak, C. E.; Nam, C. Y.; Pratum, T. K.; Bussell, M. E. *J. Catal.* **2010**, *276*, 249.

(28) Kanda, Y.; Temma, C.; Nakata, K.; Kobayashi, T.; Sugioka, M.; Uemichi, Y. *Appl. Catal., A* **2010**, *386*, 171.

(29) Shi, G.; Shen, J. *J. Mater. Chem.* **2009**, *19*, 2295.

(30) Guan, Q.; Lei, W.; Zhang, M.; Tao, K. *J. Catal.* **2009**, *263*, 1.

(31) Guan, Q.; Li, W. *J. Catal.* **2010**, *271*, 413.

(32) *JCPDS Powder Diffraction File*; International Centre for Diffraction Data: Swarthmore, PA, 2000.

(33) Gopalakrishnan, J.; Pandey, S.; Rangan, K. K. *Chem. Mater.* **1997**, *9*, 2113.

(34) Lukehart, C. M.; Milne, B. *Chem. Mater.* **1998**, *10*, 903.

(35) Schulz, H.; Rahman, N. M. *Stud. Surf. Sci. Catal.* **1993**, *75*, 585.

(36) Sitthisa, S.; Pham, T.; Prasomsri, T.; Sooknoi, T.; Mallinson, R. G.; Resasco, D. E. *J. Catal.* **2011**, *280*, 17.

(37) Avery, N. R.; Weinberg, W. H.; Anton, A. B.; Toby, B. H. *Phys. Rev. Lett.* **1983**, *51*, 682.

(38) Anton, A. B.; Avery, N. R.; Toby, B. H.; Weinberg, W. H. *J. Am. Chem. Soc.* **1986**, *108*, 684.

(39) Viljava, T.-R.; Komulainen, R. S.; Krause, A. O. I. *Catal. Today* **2000**, *60*, 83.